# Path Following of Underactuated Marine Surface Vessels in the Presence of Unknown Ocean Currents

Signe Moe[1], Walter Caharija[1], Kristin Y. Pettersen[1] and Ingrid Schjølberg[2]

*Abstract*— **Unmanned marine crafts constitute a priority area within several fields of study, and there are still many challenges related to making such vessels autonomous. A basic task of an autonomous marine craft is to follow a general path in the presence of unknown ocean currents. This paper presents a method to achieve this for surface vessels. The results are an extension of the results in [1] regarding path following of space curves when no ocean currents are present, and introduce a virtual Serret-Frenet reference frame that is anchored in and propagates along the desired path. The closed-loop system consists of an ocean current observer, a guidance law, a controller and an update law to drive the Serret-Frenet frame along the path, and is shown to be UGAS. Simulation results are presented to verify the theoretical results.**

## I. INTRODUCTION

The use of unmanned marine vehicles is rapidly increasing within several fields, such as marine biology, environmental monitoring, seafloor mapping, oceanography, military use and in the oil and gas industry. Hence, guidance and control of such autonomous crafts is a priority area within the marine control research community. This paper addresses a fundamental and highly applicable task for an autonomous underactuated surface vessel, namely path following of a general path in the presence of unknown ocean currents. Path following is a motion control scenario where the ship has to follow a predefined path without any time constraints [2]-[4].

A commonly used approach for path following is the Line of Sight (LOS) method [2],[5]-[8]. LOS is a guidance law allowing path following of general paths. However, it is most efficient when dealing with geometrically simple paths such as straight lines or circles. In the case of general, parameterized paths this method can be computationally challenging [9]. Furthermore, this control approach is susceptible to environmental disturbances such as ocean currents, waves and wind: path deviation and convergence problems will occur if the vessel is affected by environmental disturbances [10]. Integral action has been added to the LOS guidance law for marine vehicles in [10]-[14] allowing the vehicle in question to converge to and follow a straight line path in the presence of unknown ocean currents. To achieve this, the ship is allowed to side-slip to compensate for the ocean current. In [12] the steady state of the marine vessel is used to estimate the ocean current magnitude and direction. In [1] a control method based on Serret-Frenet equations for path following of general paths for both surface and underwater vehicles is proposed. However, this method does not take ocean current into account.

This paper aims at extending the control method of Børhaug [1] to obtain path following of general paths for underactuated surface vessels also under the influence of unknown ocean currents. This is achieved by expanding the guidance law in [1] and combining it with an ocean current observer described in [15]. By doing so the current is compensated for and path following is achieved asymptotically for general continuously differentiable paths. Using cascaded systems theory, the resulting closed-loop system is proved to be uniformly globally asymptotically stable (UGAS) [16]. The proposed method is similar and closely related to both LOS with integral effect in [12] and the control method of Børhaug [1], but is more general and has a wider range of applications. For instance, if no ocean current is present, the method presented in this paper will give the same result as that of Børhaug in [1]. Furthermore, if the desired path is a straight line and the ship in question is affected by current, the proposed control method ensures convergence to the same steady state side slip angle as the integral LOS method in [12].

This paper is organized as follows: Section 2 presents the model of the surface vessel and Section 3 defines the control objective. Section 4 contains the control system that solves the path following task. The stability of the closed loop system is analyzed in Section 5. Simulation results are given in Section 6 and conclusions are given in Section 7.

## II. VEHICLE MODEL

This section presents the 3-DOF surface vessel maneuvering model that is considered and the assumptions on which this is based.

### A. Model Assumptions

*Assumption 1.* The motion of the ship is described by 3 degrees of freedom (DOF), that is surge, sway and yaw.
*Assumption 2.* The ship is port-starboard symmetric.
*Assumption 3.* The body-fixed coordinate frame $b$ is located in a point $(x_g^\star, 0)$ from the vehicle's center of gravity (CG) along the center-line of the ship, where $x_g^\star$ is to be defined later.
*Remark 1.* The body-fixed coordinate system can always be translated to the required location $x_g^\star$ [2].
*Assumption 4.* The hydrodynamic damping is linear.

[1]S.Moe, W. Caharija and K.Y.Pettersen are with the Center for Autonomous Marine Operations and Systems (AMOS), at The Department of Engineering Cybernetics, Norwegian University of Science and Technology (NTNU), Trondheim, Norway {signe.moe, kristin.y.pettersen}@itk.ntnu.no

[2]I.Schjølberg is with AMOS, at the Department of Marine Technology, NTNU, Trondheim, Norway ingrid.schjolberg@ntnu.no

*Remark 2.* Nonlinear damping is not considered in order to reduce the complexity of the controllers. However, the passive nature of the non-linear hydrodynamic damping forces should enhance the directional stability of the ship.

*Assumption 5.* The ocean current in the inertial frame $i$ $\boldsymbol{V}_c \triangleq [V_x, V_y, 0]^T$ is constant, irrotational and bounded. Hence there exists a constant $V_{\max} > 0$ such that $V_{\max} > \sqrt{V_x^2 + V_y^2}$.

### B. The Vessel Model

The state of the surface vessel is given by the vector $\boldsymbol{\eta} \triangleq [x, y, \psi]^T$ and describes the position $(x, y)$ and the orientation $\psi$ of the vehicle with respect to the inertial frame $i$. The vector $\boldsymbol{\nu} \triangleq [u, v, r]^T$ contains the linear and angular velocities of the ship defined in the body-fixed frame $b$, where $u$ is the surge velocity, $v$ is the sway velocity and $r$ is the yaw rate. The ocean current velocity in the body frame $b$, $\boldsymbol{\nu}_c \triangleq [u_c, v_c, 0]^T$, is obtained from $\boldsymbol{\nu}_c = \boldsymbol{R}^T(\psi)[V_x, V_y, 0]^T$, where $\boldsymbol{R}(\psi)$ is defined as

$$\boldsymbol{R}(\psi) \triangleq \begin{bmatrix} \cos(\psi) & -\sin(\psi) & 0 \\ \sin(\psi) & \cos(\psi) & 0 \\ 0 & 0 & 1 \end{bmatrix}. \tag{1}$$

The relative velocity $\boldsymbol{\nu}_r \triangleq \boldsymbol{\nu} - \boldsymbol{\nu}_c = [u_r, v_r, r]^T$ is defined in the body frame $b$.

The following 3-DOF maneuvering model is considered [2], [12]:

$$\begin{aligned} \dot{\boldsymbol{\eta}} &= \boldsymbol{R}(\psi)\boldsymbol{\nu}_r + [V_x, V_y, 0]^T \\ \boldsymbol{M}\dot{\boldsymbol{\nu}}_r + \boldsymbol{C}(\boldsymbol{\nu}_r)\boldsymbol{\nu}_r + \boldsymbol{D}\boldsymbol{\nu}_r &= \boldsymbol{B}\boldsymbol{f} \end{aligned} \tag{2}$$

The vector $\boldsymbol{f} \triangleq [T, \delta]^T$ contains the control inputs: $T$ is the thruster force and $\delta$ is the rudder angle. The mass and inertia matrix $\boldsymbol{M}$ is symmetric and positive definite and includes hydrodynamic added mass. $\boldsymbol{C}$ is the Coriolis and centripetal matrix and $\boldsymbol{D}$ is the positive definite hydrodynamic damping matrix. $\boldsymbol{B} \in \mathbb{R}^{3\times 2}$ is the actuator configuration matrix. The matrices have the following structure:

$$\begin{aligned} \boldsymbol{M} &\triangleq \begin{bmatrix} m_{11} & 0 & 0 \\ 0 & m_{22} & m_{23} \\ 0 & m_{23} & m_{33} \end{bmatrix}, \ \boldsymbol{D} \triangleq \begin{bmatrix} d_{11} & 0 & 0 \\ 0 & d_{22} & d_{23} \\ 0 & d_{32} & d_{33} \end{bmatrix}, \ \boldsymbol{B} \triangleq \begin{bmatrix} b_{11} & 0 \\ 0 & b_{22} \\ 0 & b_{32} \end{bmatrix} \\ \boldsymbol{C}(\boldsymbol{\nu}_r) &\triangleq \begin{bmatrix} 0 & 0 & -m_{22}v_r - m_{23}r \\ 0 & 0 & m_{11}u_r \\ m_{22}v_r + m_{23}r & -m_{11}u_r & 0 \end{bmatrix} \end{aligned} \tag{3}$$

Assumptions 1-4 justify the structure of $\boldsymbol{M}$ and $\boldsymbol{D}$ and the structure of $\boldsymbol{C}$ is obtained as described in [2]. Furthermore, the point $x_g^\star$ from Assumption 3 is chosen so that $\boldsymbol{M}^{-1}\boldsymbol{B}\boldsymbol{f} = [\tau_u, 0, \tau_r]^T$. The point $(x_g^\star, 0)$ exists for all port-starboard symmetric ships [10].

*Remark 3.* It is shown in [2] that since the ocean current is constant and irrotational in $i$, the ship can be described by the 3-DOF maneuvering model in (2).

### C. The Model in Component Form

For the control design is it useful to expand (2) into component form:

$$\begin{aligned} \dot{x} &= \cos(\psi)u_r - \sin(\psi)v_r + V_x, \\ \dot{y} &= \sin(\psi)u_r + \cos(\psi)v_r + V_y, \\ \dot{\psi} &= r, \\ \dot{u}_r &= F_{u_r}(v_r, t) - \frac{d_{11}}{m_{11}}u_r + \tau_u, \\ \dot{v}_r &= X(u_r)r + Y(u_r)v_r, \\ \dot{r} &= F_r(u_r, v_r, r) + \tau_r \end{aligned} \tag{4}$$

The expressions for $F_{u_r}$, $X(u_r)$, $Y(u_r)$ and $F_r(u_r, v_r, r)$ are given in the Appendix.

## III. CONTROL OBJECTIVE

This section formalizes the control problem solved in this paper: The control system should make the vessel follow a given smooth path $C$ and maintain a desired constant relative surge velocity $U_{rd} > 0$ in the presence of unknown constant irrotational ocean currents. $C$ is parametrized with respect to the inertial frame $i$ as a function of the arc length $s$: $C \triangleq \{(x_f(s), y_f(s), \psi_f(s))\}$. To accomplish this, a virtual reference Serret-Frenet frame $f$ is introduced (see Figure 1). This is anchored in and propagates along $C$ with instantaneous speed $\dot{s}$. The notation $X^{U_{rd}} \triangleq |X(U_{rd})|$ and $Y^{U_{rd}} \triangleq |Y(U_{rd})|$ is used.

*Assumption 6.* The functions $X(u_r)$ and $Y(u_r)$ satisfy $Y(U_{rd}) < 0$, $-U_{rd} + a \leq X(U_{rd}) \leq X^{U_{rd}}$, where $a$ is a positive constant.

*Remark 4.* $Y(U_{rd}) < 0$ is a natural assumption since $Y(U_{rd}) = 0$ would imply that the supply ship is undamped in sway and $Y(U_{rd}) > 0$ would imply that some small perturbation in sway would result in an accelerating sway velocity for $u_r = U_{rd}$ [1]. In reality it would indicate that a push in the sway-direction would result in a constantly increasing sway velocity, a response that is physically impossible. $-U_{rd} + a \leq X(U_{rd}) \leq X^{U_{rd}}$ is not a very strict demand since $U_{rd}$ is a design parameter that can be chosen to fulfill this inequality.

Denoting $x_{b/f}$ and $y_{b/f}$ as the position of the body frame $b$ relative to the Serret-Frenet frame $f$ and $\psi_{b/f} \triangleq \psi - \psi_f$ as the relative orientation of the vessel relative to the $f$-frame, the control objectives can be formalized as follows:

$$\begin{aligned} \lim_{t\to\infty} x_{b/f}(t) &= 0 \\ \lim_{t\to\infty} y_{b/f}(t) &= 0 \\ \lim_{t\to\infty} u_r(t) &= U_{rd} \end{aligned} \tag{5}$$

As Figure 1 shows, driving $x_{b/f}$ and $y_{b/f}$ to zero will result in the vessel converging to the path. Since the Serret-Frenet frame is virtual, we are free to choose the evolution $\dot{s}$ of this frame along the path. In this paper the relative surge velocity $u_r$ is controlled. As such, the total path following speed $U = \sqrt{u^2 + v^2}$ is unconstrained and unknown. For

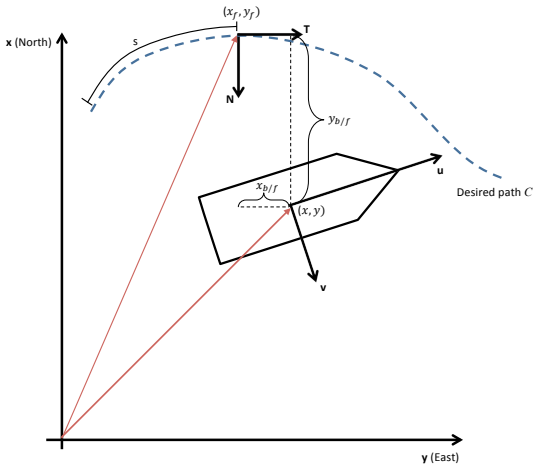


Fig. 1. The inertial frame x-axis points north and the y-axis points east. The Serret-Frenet frame has axes denoted $T$ and $N$ and is anchored in the desired path. The position of this frame relative to the inertial frame is $(x_f, y_f)$. The body frame is fixed on the marine surface vessel. The position of the body frame relative to the inertial frame and Serret-Frenet frame is denoted $(x, y)$ and $(x_{b/f}, y_{b/f})$ respectively.

speed profile planning/tracking scenarios, this is not ideal. On the other hand, controlling the relative velocity of the vessel gives direct control of energy consumption and any lift forces due to transom stern effects.

*Assumption 7.* The propulsion system is rated with power and thrust capasity such that $U_{rd}$ satisfies $0 \leq V_{\max} < U_{rd}$.

*Remark 5.* For most surface vessels Assumption 7 is easily fulfilled since their propulsion systems are designed to give much more than 5 meters per second of relative speed $U_{rd}$. The ocean current has usually an intensity of less than 1 meter per second.

## IV. THE CONTROL SYSTEM

In this section a control system that solves the control objectives in (5) is presented. This includes a current observer, a guidance law, an update law and surge and yaw controllers.

### A. Ocean Current Observer

The current estimator for a surface ship is given in [15]. The observer is a Luenberger type observer based on the model in (4). In addition to estimating the current components $V_x$ and $V_y$, it gives estimates of the known states $x$ and $y$ that can be compared to the actual states. The observer is given below:

$$\begin{aligned} \dot{\hat{x}} &= \cos(\psi)u_r - \sin(\psi)v_r + \hat{V}_x + k_{x_1}\tilde{x}, \\ \dot{\hat{y}} &= \sin(\psi)u_r + \cos(\psi)v_r + \hat{V}_y + k_{y_1}\tilde{y}, \\ \dot{\hat{V}}_x &= k_{x_2}\tilde{x}, \\ \dot{\hat{V}}_y &= k_{y_2}\tilde{y}, \end{aligned} \tag{6}$$

where $\hat{x}$, $\hat{y}$, $\hat{V}_x$ and $\hat{V}_y$ are the estimates of $x$, $y$, $V_x$ and $V_y$.

*Assumption 8.* The current estimator is saturated in accordance with Assumption 5: $\sqrt{\hat{V}_x^2 + \hat{V}_y^2} \leq V_{\max} < U_{rd}$.

*Remark 6.* The saturation is placed on the estimated current after the feedback loop so the saturation does not affect the stability of the observer.

In (6), $\tilde{x} \triangleq x - \hat{x}$, $\tilde{y} \triangleq y - \hat{y}$, $\tilde{V}_x \triangleq V_x - \hat{V}_x$ and $\tilde{V}_y \triangleq V_y - \hat{V}_y$. If the constant gain parameters $k_{x_1}$, $k_{y_1}$, $k_{x_2}$ and $k_{y_2}$ are greater than zero, the errors $\tilde{x}$, $\tilde{y}$, $\tilde{V}_x$ and $\tilde{V}_y$ will approach zero with global exponential stability [15].

In this paper, the following notation is used for the ocean current and ocean current estimate in the $f$-frame:

$$\begin{aligned} V_x^f &= \cos(\psi_f)V_x + \sin(\psi_f)V_y \\ V_y^f &= -\sin(\psi_f)V_x + \cos(\psi_f)V_y \\ \hat{V}_x^f &= \cos(\psi_f)\hat{V}_x + \sin(\psi_f)\hat{V}_y \\ \hat{V}_y^f &= -\sin(\psi_f)\hat{V}_x + \cos(\psi_f)\hat{V}_y \end{aligned} \tag{7}$$

### B. Guidance and Update Laws

Equation (8) and (9) contain the update law used to drive the $f$-frame forward along the desired path and the guidance law providing the yaw controller with its reference, respectively.

$$\dot{s} = \underbrace{\sqrt{U_{rd}^2 + v_r^2}}_{\triangleq U_c} \frac{\sqrt{\Delta^2 + x_{b/f}^2} + x_{b/f}}{\sqrt{\Delta^2 + x_{b/f}^2 + (y_{b/f} + g)^2}} + \hat{V}_x^f, \tag{8}$$

$$\psi_{ref} = \psi_f - \arctan\left(\frac{v_r}{U_{rd}}\right) - \arctan\left(\frac{y_{b/f} + g}{\sqrt{\Delta^2 + x_{b/f}^2}}\right), \tag{9}$$

where $g$ is the solution to the second-order equation

$$\underbrace{(\hat{V}_y^{f^2} - U_c^2)}_{a} g^2 + 2\underbrace{\hat{V}_y^{f^2} y_{b/f}}_{b} g + \underbrace{\hat{V}_y^{f^2}\left(\Delta^2 + x_{b/f}^2 + y_{b/f}^2\right)}_{c} = 0, \tag{10}$$

and $\Delta > 0$ is a design parameter.

*Assumption 9.* The parameter $\Delta$ satisfies $\Delta > \frac{\frac{3}{2}X^{U_{rd}}}{Y^{U_{rd}} - 3X^{U_{rd}}\kappa_{\max}}$.

*Assumption 10.* The curvature of the desired path is bounded such that $\kappa_{\max} \triangleq \max_{s\in\mathbb{R}} |\kappa(s)| < \frac{1}{3}\frac{Y^{U_{rd}}}{X^{U_{rd}}}$.

*Remark 7.* Assumptions 7 and 8 ensure that the solution(s) of (10) are real and finite.

*Remark 8.* Assumptions 6, 9 and 10 are used to prove boundedness for $v_r$, see section V.

Equation (10) is a second order equation with parameters $(a, 2b, c)$ and thus it has two possible solutions:

$$\begin{aligned} g_1 &\triangleq \frac{-b - \sqrt{b^2 - ac}}{a}, \\ g_2 &\triangleq \frac{-b + \sqrt{b^2 - ac}}{a}. \end{aligned} \tag{11}$$

To prove stability, $g$ must have the same sign as $\hat{V}_y^f$ (this will be shown in Section V). By simple analysis and Assumptions 7 and 8, $a < 0$ and $c \geq 0$. Furthermore, as time progresses $y_{b/f}$ and consequently $b$ approach zero. As such, $g_1$ will

always be positive ($\geq 0$) and $g_2$ will always be negative ($\leq 0$) and $g$ is thus chosen as follows:

$$g = \begin{cases} g_1 & \hat{V}_y^f \geq 0 \\ g_2 & \hat{V}_y^f < 0 \end{cases} \tag{12}$$

### C. Surge and Yaw Controllers

A feedback linearizing P-controller is used to ensure tracking of the desired relative surge velocity $u_{rd}(t)$.

$$\tau_u = -F_{u_r}(v_r, r) + \frac{d_{11}}{m_{11}} u_{rd} + \dot{u}_{rd} - k_{u_r}(u_r - u_{rd}). \tag{13}$$

The gain $k_{u_r} > 0$ is constant. From (4) we see that the controller (13) guarantees exponential tracking of $u_{rd}(t)$. For the control problem considered in this paper, $u_{rd}(t) \triangleq U_{rd}$. Part of the damping is not canceled in order to guarantee some robustness with respect to model uncertainties. Furthermore, a feedback linearizing PD-controller is used to track the desired yaw angle $\psi_d$. In this case $\psi_d(t) = \psi_{ref}(t)$ is provided by the guidance law (9) and $\dot{\psi}_d(t)$ is calculated by taking the time derivative of $\psi_d(t)$.

$$\tau_r = -F_r(u_r, v_r, r) + \ddot{\psi}_d - k_\psi(\psi - \psi_d) - k_r(\dot{\psi} - \dot{\psi}_d). \tag{14}$$

$k_\psi$ and $k_r$ are strictly positive constant controller gains. From (4) we see that the controller (14) ensures exponential tracking of $\psi_d$ and $\dot{\psi}_d$.

### D. State Measurements

The control system proposed in this papers assumes that $\boldsymbol{\eta}$ and $\boldsymbol{\nu_r}$ are measured. Ships are usually equipped with a large variety of sensors that combined provide sensor data to estimate the vessel state [2]. For instance, absolute position/velocity can be estimated using an Inertial Measurement Unit (IMU) and a GPS receiver. To measure relative velocity, Acoustic Doppler Current Profilers (ADCP), Pitometer Logs and Paddle meters can be used. ADCP uses acoustic measurements to capture the relative velocity. The Pitometer log compares the dynamic and static pressures of the fluid, and the Paddle meter measures spin velocity of a paddle driven by the flow itself.

The proposed update law (8) and guidance law (9) depends on an estimate of the ocean current. One possibility would be to simply estimate it as the difference between the measured absolute and relative velocity. However, the suggested ocean current observer (6) depends only on position and relative velocity measurements, as do the controllers, update law and guidance law. Relative velocity logs such as ADCPs or Pitometers are expected to give more reliable results than GPS based absolute speed measurements [12]. Therefore, the proposed observer increases the robustness of the control system.

Since the controllers (13) and (14) depend on the time derivative of the reference signals, they are susceptible to measurement noise. Thus, reliable sensors with minimal measurement noise are crucial in a real-life application of these controllers. The effects of measurement noise can also be minimized by utilizing a low-pass filter on the sensor data.

## V. MAIN RESULT

This section presents the conditions under which the proposed control system achieves the control objectives (5).

*Theorem 1.* Given an underactuated surface vessel described by the dynamical system (4). If Assumptions 5-10 hold, then the controllers (13) and (14), where $u_{rd}(t) \triangleq U_{rd}$ and $\psi_d$ is given by (9), guarantee achievement of the control objectives (5).

**Proof.** By defining $\tilde{u}_r \triangleq u_r - U_{rd}$, $\tilde{\psi} \triangleq \psi - \psi_d$ and $\dot{\tilde{\psi}} \triangleq \dot{\psi} - \dot{\psi}_d$ and combining the system surge and yaw dynamics (4) with the control laws (13) and (14) we find the expressions for the error dynamics. Similarly, this can be done for the observer errors $\tilde{x}$, $\tilde{y}$, $\tilde{V}_x$ and $\tilde{V}_y$. First, consider the vector $\boldsymbol{\xi} \triangleq \left[\tilde{u}_r, \tilde{\psi}, \dot{\tilde{\psi}}, \tilde{V}_x, \tilde{V}_y, \tilde{x}, \tilde{y}\right]^T$.

$$\dot{\boldsymbol{\xi}} = \begin{bmatrix} -(k_{u_r} + \frac{d_{11}}{m_{11}}) & 0 & 0 & 0 & 0 & 0 & 0 \\ 0 & 0 & 1 & 0 & 0 & 0 & 0 \\ 0 & 0 & -k_\psi & -k_r & 0 & 0 & 0 \\ 0 & 0 & 0 & 0 & 0 & -k_{x_2} & 0 \\ 0 & 0 & 0 & 0 & 0 & 0 & -k_{y_2} \\ 0 & 0 & 0 & 1 & 0 & -k_{x_1} & 0 \\ 0 & 0 & 0 & 0 & 1 & 0 & -k_{y_1} \end{bmatrix} \boldsymbol{\xi} \triangleq \boldsymbol{\Lambda}\boldsymbol{\xi} \tag{15}$$

The system (15) is linear and time-invariant. Furthermore, since all controller and observer gains and $\frac{d_{11}}{m_{11}}$ are strictly positive, $\boldsymbol{\Lambda}$ is Hurwitz and the origin $\boldsymbol{\xi} = \mathbf{0}$ of (15) is uniformly globally exponentially stable (UGES).

The dynamics of the body frame relative to the Serret-Frenet can be expressed as follows [1]:

$$\begin{aligned} \begin{bmatrix} \dot{x}_{b/f} \\ y_{b/f} \end{bmatrix} = \begin{bmatrix} \cos(\psi_{b/f}) & -\sin(\psi_{b/f}) \\ \sin(\psi_{b/f}) & \cos(\psi_{b/f}) \end{bmatrix} \begin{bmatrix} u \\ v \end{bmatrix} - \begin{bmatrix} \dot{s} \\ 0 \end{bmatrix} \\ - \dot{s} \begin{bmatrix} 0 & -\kappa \\ \kappa & 0 \end{bmatrix} \begin{bmatrix} x_{b/f} \\ y_{b/f} \end{bmatrix}. \end{aligned} \tag{16}$$

This can be rewritten as:

$$\begin{aligned} \begin{bmatrix} \dot{x}_{b/f} \\ y_{b/f} \end{bmatrix} = \begin{bmatrix} \cos(\psi_{b/f}) & -\sin(\psi_{b/f}) \\ \sin(\psi_{b/f}) & \cos(\psi_{b/f}) \end{bmatrix} \begin{bmatrix} u_r \\ v_r \end{bmatrix} - \begin{bmatrix} \dot{s} \\ 0 \end{bmatrix} \\ - \dot{s} \begin{bmatrix} 0 & -\kappa \\ \kappa & 0 \end{bmatrix} \begin{bmatrix} x_{b/f} \\ y_{b/f} \end{bmatrix} + \begin{bmatrix} \cos(\psi_f) & \sin(\psi_f) \\ -\sin(\psi_f) & \cos(\psi_f) \end{bmatrix} \begin{bmatrix} V_x \\ V_y \end{bmatrix}. \end{aligned} \tag{17}$$

Using the expressions for the current observer (6), the update law (8), guidance law (9) and controllers (13-14), (17) can be expressed as:

$$\begin{bmatrix} \dot{x}_{b/f} \\ \dot{y}_{b/f} \end{bmatrix} = \begin{bmatrix} -U_c \frac{x_{b/f}}{\sqrt{\Delta^2 + x_{b/f}^2 + (y_{b/f}+g)^2}} \\ -U_c \frac{y_{b/f}}{\sqrt{\Delta^2 + x_{b/f}^2 + (y_{b/f}+g)^2}} \end{bmatrix} - \dot{s} \begin{bmatrix} 0 & -\kappa \\ \kappa & 0 \end{bmatrix} \begin{bmatrix} x_{b/f} \\ y_{b/f} \end{bmatrix} + \boldsymbol{H}(t, U_c, \boldsymbol{\xi})\boldsymbol{\xi}, \tag{18}$$

$$\boldsymbol{H}(t, U_c, \boldsymbol{\xi}) = \begin{bmatrix} \cos(\psi_{fb}) & \sin(\psi_{fb}) \\ h_1(t, U_c, \boldsymbol{\xi}) & h_2(t, U_c, \boldsymbol{\xi}) \\ 0 & 0 \\ \cos(\psi_f) & -\sin(\psi_f) \\ \sin(\psi_f) & \cos(\psi_f) \\ 0 & 0 \\ 0 & 0 \end{bmatrix}^T, \tag{19}$$

$$h_1(t,U_c,\boldsymbol{\xi}) = \frac{\cos(\tilde{\psi})-1}{\tilde{\psi}} U_c \frac{\sqrt{\Delta^2+x_{b/f}^2}}{\sqrt{\Delta^2+x_{b/f}^2+(y_{b/f}+g)^2}} + \frac{\sin(\tilde{\psi})}{\tilde{\psi}} U_c \frac{y_{b/f}+g}{\sqrt{\Delta^2+x_{b/f}^2+(y_{b/f}+g)^2}},$$
$$h_2(t,U_c,\boldsymbol{\xi}) = \frac{\sin(\tilde{\psi})}{\tilde{\psi}} U_c \frac{\sqrt{\Delta^2+x_{b/f}^2}}{\sqrt{\Delta^2+x_{b/f}^2+(y_{b/f}+g)^2}} - \frac{\cos(\tilde{\psi})-1}{\tilde{\psi}} U_c \frac{y_{b/f}+g}{\sqrt{\Delta^2+x_{b/f}^2+(y_{b/f}+g)^2}}. \tag{20}$$

The system in (18) and the dynamics of $\boldsymbol{\xi}$ (15) can be seen as a cascaded system where the error dynamics (15) perturbs the nominal system (21) through the term $\boldsymbol{H}(t,U_c,\boldsymbol{\xi})\boldsymbol{\xi}$.

$$\begin{bmatrix}\dot{x}_{b/f}\\ \dot{y}_{b/f}\end{bmatrix} = \begin{bmatrix}-U_c \frac{x_{b/f}}{\sqrt{\Delta^2+x_{b/f}^2+(y_{b/f}+g)^2}}\\ -U_c \frac{y_{b/f}}{\sqrt{\Delta^2+x_{b/f}^2+(y_{b/f}+g)^2}}\end{bmatrix} - \dot{s}\begin{bmatrix}0 & -\kappa\\ \kappa & 0\end{bmatrix}\begin{bmatrix}x_{b/f}\\ y_{b/f}\end{bmatrix} \tag{21}$$

The stability of the nominal system (21) can be proven using the quadratic positive definite Lyapunov function $V = \frac{1}{2}(x_{b/f}^2+y_{b/f}^2)$.

$$\begin{aligned}\dot{V} &= \dot{x}_{b/f}x_{b/f}+\dot{y}_{b/f}y_{b/f}\\ &= -U_c\frac{x_{b/f}^2+y_{b/f}^2}{\sqrt{\Delta^2+x_{b/f}^2+(y_{b/f}+g)^2}} + \dot{s}\kappa x_{b/f}y_{b/f} - \dot{s}\kappa x_{b/f}y_{b/f}\\ &\leq -U_{rd}\frac{x_{b/f}^2+y_{b/f}^2}{\sqrt{\Delta^2+x_{b/f}^2+(y_{b/f}+g)^2}}\\ &\triangleq W(x_{b/f},y_{b/f},g) < 0\end{aligned} \tag{22}$$

$\dot{V}$ is negative definite and thus the nominal system (21) is UGAS. Furthermore, the interconnection matrix $\boldsymbol{H}(t,U_c,\boldsymbol{\xi})$ is bounded for bounded $U_c = \sqrt{U_{rd}^2+v_r^2}$, which in turn is bounded for bounded $v_r$. If Assumptions 6, 9 and 10 are fulfilled, $v_r$ is shown to be uniformly bounded follwing the same procedure as [1]. Theorem 2 from [16] can then be applied to prove stability of the entire cascaded system (15) and (18). In particular, the nominal system is UGAS with a quadratic Lyapunov-function. The error dynamics is UGES, and the interconnection matrix $\boldsymbol{H}$ is globally bounded. Consequently, the cascaded system in (15) and (18) is UGAS, and $x_{b/f}$, $y_{b/f}$ and $\tilde{u}_r$ converge to zero with uniform global asymptotic stability. Thus the control objectives are satisfied.

## VI. SIMULATIONS

This section presents simulation results when the desired path is a straight line and a circular path, respectively. Numeric values for the ship model is given in [17]. In all simulations, the following numeric values are used:

$$\begin{array}{llll} U_{rd}=5\frac{m}{s} & \boldsymbol{V}_c=[-1,1.2]^T\frac{m}{s} & V_{\max}=4\frac{m}{s} & \Delta=50m\\ k_{u_r}=0.1s^{-1} & k_\psi=0.04s^{-2} & k_r=0.1s^{-1} & \\ k_{x_1}=4s^{-1} & k_{x_2}=0.05s^{-2} & k_{y_1}=4s^{-1} & k_{y_2}=0.05s^{-2}\end{array}$$

The desired path $C$ is parametrized as below.

***Line***
$$\begin{aligned}x_f(s) &= s\cos(\psi_f(s))\\ y_f(s) &= s\sin(\psi_f(s))\\ \psi_f(s) &= 40^\circ\end{aligned} \tag{23}$$

***Circle***
$$\begin{aligned}x_f(s) &= R\cos(\frac{s}{R})+C_1\\ y_f(s) &= R\sin(\frac{s}{R})+C_2\\ \psi_f(s) &= \frac{s}{R}+\frac{\pi}{2}\\ R &= 400m\\ C_1 &= 0m\\ C_2 &= 800m\end{aligned} \tag{24}$$

The two paths both have a constant curvature, $\kappa(s)=0$ and $\kappa(s)=\frac{1}{R}=0.0025$, respectively. With $U_{rd}=5\frac{m}{s}$, we find that $X(U_{rd})=-X^{U_{rd}}=-2.8480$ and $Y(U_{rd})=-Y^{U_{rd}}=-0.3774$. As such, it is trivial to verify that all Assumptions are fulfilled. Simulation results are shown in Figure 2 and 3, and confirm that the control objectives are fulfilled. The ship converges to the desired path and $x_{b/f}$ and $y_{b/f}$ converge to 0. Furthermore, the controllers ensure that $u_r(t)$ and $\psi(t)$ converge to and track their respective references. Finally, the current observer correctly estimates the ocean currents. Figure 2 and 3 also confirm the importance of the current observer: Path following coincides with correct current estimation. Furthermore, all simulations were conducted with an appropriate saturation on the thruster force $T$ and the rudder angle $\delta$, confirming that the control system is applicable in a real-life scenario.

## VII. CONCLUSIONS

In this paper a guidance and control system for an underactuated surface vessel is developed to solve the control objective of making the vessel follow a general path in the presence of unknown ocean currents. The paper is motivated by the path following methods of [1], and by expanding these guidance and update laws and combining them with an ocean current observer [15], convergence to the desired path is achieved with UGAS stability properties under explicit conditions. Simulation results verify the theoretical results.

Future work includes simulating with measurement noise, model uncertainty, slowly-varying currents and testing in the field to validate the method with experimental results.

## APPENDIX

$$F_{u_r}(v_r,r) = \frac{m_{22}v_r+m_{23}r}{m_{11}}r \tag{25}$$

$$X(u_r) = \frac{{m_{23}}^2-m_{11}m_{33}}{m_{22}m_{33}-{m_{23}}^2}u_r + \frac{d_{33}m_{23}-d_{23}m_{33}}{m_{22}m_{33}-{m_{23}}^2} \tag{26}$$

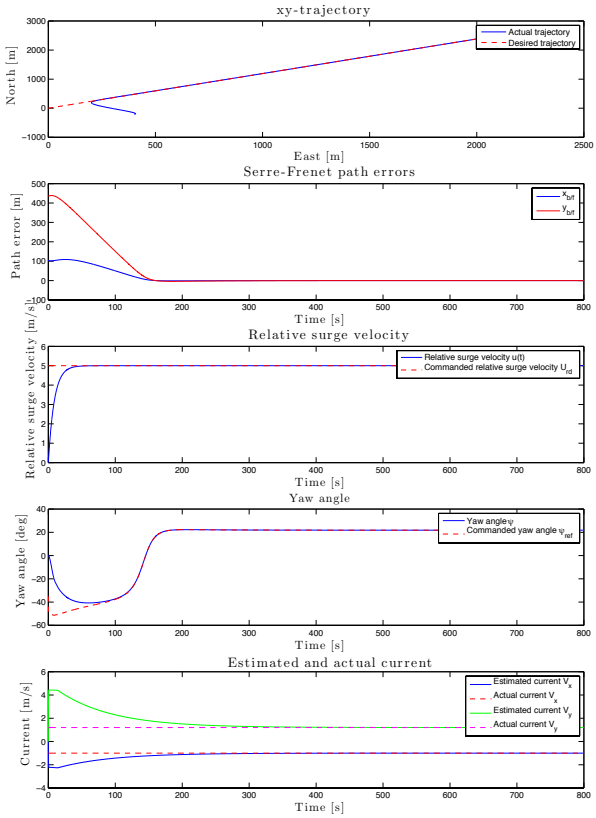


Fig. 2. Simulations results for straight line path following in the presence of unknown ocean currents.

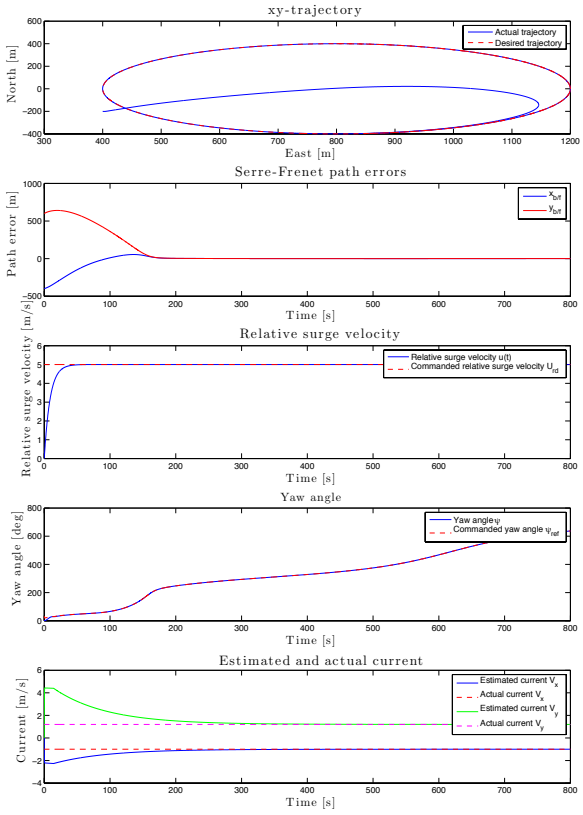


Fig. 3. Simulations results for circular line path following in the presence of unknown ocean currents.

$$Y(u_r) = \frac{m_{22}m_{23} - m_{11}m_{23}}{m_{22}m_{33} - {m_{23}}^2}u_r - \frac{d_{22}m_{33} - d_{32}m_{23}}{m_{22}m_{33} - {m_{23}}^2} \tag{27}$$

$$\begin{aligned} F_r(u_r, v_r, r) = &\frac{m_{23}d_{22} - m_{22}(d_{32} + (m_{22} - m_{11})u_r)}{m_{22}m_{33} - {m_{23}}^2}v_r \\ &+ \frac{m_{23}(d_{23} + m_{11}u_r) - m_{22}(d_{33} + m_{23}u_r)}{m_{22}m_{33} - {m_{23}}^2}r \end{aligned} \tag{28}$$

## ACKNOWLEDGMENTS

This work was supported by the Research Council of Norway through the Centres of Excellence funding scheme, project number 223254.

## REFERENCES

[1] E. Børhaug and K. Pettersen, "LOS path following for underactuated underwater vehicle," *in Proc. 7th IFAC Conference on Manoeuvring and Control of Marine Craft*, Lisbon, Portugal, 2006.

[2] T. Fossen, *Handbook of Marine Craft Hydrodynamics and Motion Control*. Wiley, 2011.

[3] A. Aguiar and J. Hespanha, "Trajectory-tracking and path-following of underactuated autonomous vehicles with parametric modeling uncertainty," *IEEE Transactions on Automatic Control*, vol. 52, no. 8, pp. 1362–1379, 2007.

[4] P. Encarnao and A. M. Pascoal, "Combined trajectory tracking and path following: an application to the coordinated control of autonomous marine craft," Orlando, Florida, 2001.

[5] A. Healey and D. Lienard, "Multivariable sliding mode control for autonomous diving and steering of unmanned underwater vehicles," *IEEE Journal of Oceanic Engineering*, vol. 18, no. 3, pp. 327–339, 1993.

[6] R. Skjetne, U. Jørgensen, and A. R. Teel, "Line-of-sight path-following along regularly parametrized curves solved as a generic maneuvering problem," Orlando, Florida, 2011.

[7] P. Encarnao, A. M. Pascoal, and M. Arcak, "Path following for marine vehicles in the presence of unknown currents," Vienna, Austria, 2000.

[8] K. Y. Pettersen and E. Lefeber, "Way-point tracking control of ships," Orlando, Florida, 2001.

[9] M. Breivik and T. Fossen, "Guidance laws for planar motion control," *in Proc. 47th IEEE Conference on Decision and Control*, pp. 570 –577, Cancun, Mexico, 2008.

[10] E. Borhaug, A. Pavlov, and K. Pettersen, "Integral LOS control for path following of underactuated marine surface vessels in the presence of constant ocean currents," *in Proc. 47th IEEE Conference on Decision and Control*, pp. 4984 –4991, Cancun, Mexico, 2008.

[11] W. Caharija, K. Pettersen, J. Gravdahl, and A. Sorensen, "Topics on current compensation for path following applications of underactuated underwater vehicles," *in Proc. 9th IFAC Workshop on Navigation, Guidance and Control of Underwater Vehicles*, Porto, Portugal, 2012.

[12] W. Caharija, K. Pettersen, M. Candeloro, and A. Sorensen, "Relative Velocity Control and Integral LOS for Path Following of Underactuated Surface Vessels," *in Proc. 9th IFAC Conference on Manoeuvring and Control of Marine Craft*, Arenzano, Italy, 2012.

[13] W. Caharija, K. Pettersen, J. Gravdahl, and E. Borhaug, "Integral LOS guidance for horizontal path following of underactuated autonomous underwater vehicles in the presence of vertical ocean currents," *in Proc. American Control Conference*, Montréal, Canada, 2012.

[14] ——, "Path following of underactuated autonomous underwater vehicles in the presence of ocean currents," *in Proc. 51th IEEE Conference on Decision and Control*, Maui, Hawaii, 2012.

[15] A. P. Aguiar and A. Pascoal, "Dynamic positioning and way-point tracking of underactuated auvs in the presence of ocean currents," *in Proc. 41st IEEE Conference on Decision and Control*, Las Vegas, Nevada, 2002.

[16] E. Panteley and A. Loria, "On global uniform asymptotic stability of nonlinear time-varying systems in cascade," *Systems and Control Letters*, vol. 33, no. 2, 1998.

[17] E. Fredriksen and K. Pettersen, "Global kappa-exponential way-point manoeuvering of ships," *in Proc. IEEE Conference on Decision and Control*, Paradise Island, Bahamas, 2004.